Cancer Letters 421 (2018) 17–27

Contents lists available at ScienceDirect

Cancer Letters

journal homepage: www.elsevier.com/locate/canlet

Original Articles

Bone marrow-derived fibrocytes promote stem cell-like properties of lung cancer cells

Atsuro Saijo [a], Hisatsugu Goto [a], Mayuri Nakano [a], Atsushi Mitsuhashi [a], Yoshinori Aono [a], Masaki Hanibuchi [a], Hirohisa Ogawa [b], Hisanori Uehara [b], Kazuya Kondo [c], Yasuhiko Nishioka [a, *]

[a] Department of Respiratory Medicine and Rheumatology, Graduate School of Biomedical Sciences, Tokushima University, Tokushima, Japan
[b] Department of Pathology and Laboratory Medicine, Graduate School of Biomedical Sciences, Tokushima University, Tokushima, Japan
[c] Department of Thoracic, Endocrine Surgery and Oncology, Graduate School of Biomedical Sciences, Tokushima University, Tokushima, Japan

ARTICLE INFO

Article history:
Received 7 December 2017
Received in revised form
25 January 2018
Accepted 8 February 2018

Keywords:
Lung cancer
Cancer stem cell
Fibrocyte
Tumor microenvironment
AKT pathway

ABSTRACT

Cancer stem cells (CSCs) represent a minor population that have clonal tumor initiation and self-renewal capacity and are responsible for tumor initiation, metastasis, and therapeutic resistance. CSCs reside in niches, which are composed of diverse types of stromal cells and extracellular matrix components. These stromal cells regulate CSC-like properties by providing secreted factors or by physical contact. Fibrocytes are differentiated from bone marrow-derived $CD14^+$ monocytes and have features of both macrophages and fibroblasts. Accumulating evidence has suggested that stromal fibrocytes might promote cancer progression. However, the role of fibrocytes in the CSC niches has not been revealed. We herein report that human fibrocytes enhanced the CSC-like properties of lung cancer cells through secreted factors, including osteopontin, CC-chemokine ligand 18, and plasminogen activator inhibitor-1. The PIK3K/AKT pathway was critical for fibrocytes to mediate the CSC-like functions of lung cancer cells. In human lung cancer specimens, the number of tumor-infiltrated fibrocytes was correlated with high expression of CSC-associated protein in cancer cells. These results suggest that fibrocytes may be a novel cell population that regulates the CSC-like properties of lung cancer cells in the CSC niches.

1. Introduction

Tumor tissue is not a simple aggregate of homogenous cancer cells; rather, it is a complex cluster of various cell types, including not only cancer cells but also stromal cells [1]. Even among cancer cells, distinct phenotypic statuses that differ in functional attributes often exist, which makes it difficult to control their growth. In such a situation of tumor-cell heterogeneity, cancer stem cells (CSCs) represent a minor but important population that have been shown to have clonal tumor initiation and self-renewal capacity [2], and these stem cell-like properties are thought to be responsible for tumor metastasis, recurrence, and therapeutic resistance [3].

Thus far, various attempts have been made to target CSCs in order to regulate the progression of cancer; however, applicable treatment strategies have yet to be developed. This may be due in part to the fact that CSCs reside in and are protected by niches comprised of various stromal cells, providing desirable condition to CSCs by direct cell-cell contact or by secreted factors. In this regard, it is crucial to understand how these complex and specialized environments are formed, in order to control the fate of CSCs. Among the cells that comprise the CSC niche, cancer-associated fibroblasts (CAFs), mesenchymal stem cells (MSCs), tumor-associated macrophages (TAMs), and myeloid-derived suppressor cells (MDSCs) are reported to be important for maintaining the microenvironment [3]. However, given that the composition and mechanisms underlying the CSC niche have not been fully elucidated, we hypothesized that there are still as-yet-undiscovered cellular mechanisms underlying the composition of the CSC niche.

Fibrocytes are a minor population of leukocytes that differentiate from bone-marrow derived $CD14^+$ monocytes. The distinctive feature of these cells is that they have fibroblast-like tissue remodeling properties in addition to their original inflammatory

* Corresponding author. Department of Respiratory Medicine and Rheumatology, Graduate School of Biomedical Sciences, Tokushima University, 3-18-15 Kuramoto-cho, Tokushima, 770-8503, Japan.
E-mail address: yasuhiko@tokushima-u.ac.jp (Y. Nishioka).

https://doi.org/10.1016/j.canlet.2018.02.016
0304-3835/

properties of macrophages [4]. We recently found that fibrocytes contribute to the acquired resistance to anti-VEGF therapy in lung cancer and malignant pleural mesothelioma by producing alternative angiogenic factors, such as FGF2 [5]. These results prompted us to consider that fibrocytes may also play a role in regulating cancer growth by affecting CSCs, as CSCs are deeply involved in drug resistance.

Under this hypothesis, we focused on fibrocytes as a previously unrecognized cell type involved in CSC niche.

2. Materials and methods

2.1. Cell lines

The human lung adenocarcinoma cell line A549 was purchased from the American Type Culture Collection. The human small cell lung cancer cell line SBC-5 was kindly provided by Drs. M. Tanimoto and K. Kiura (Okayama University, Okayama, Japan). These cell lines were authenticated and maintained according to previously published methods [5,6].

2.2. Reagents

The anti-mouse IL-2 receptor β-chain monoclonal antibody TM-β1 was supplied by Drs. M. Miyasaka and T. Tanaka (Osaka University, Osaka, Japan). Cisplatin was purchased from Wako Pure Chemical (Osaka, Japan). Neutralizing antibodies to Chitinase 3-like 1 (CH3L1), growth differentiation factor 15 (GDF-15), osteopontin (OPN), CC-chemokine ligand 2 (CCL-2), and CC-chemokine ligand 7 (CCL-7) were purchased from R&D Systems (Minneapolis, MN, USA). Neutralizing antibodies to MMP-9 and CC-chemokine ligand 18 (CCL-18) were purchased from Abcam (Cambridge, MA, USA). The plasminogen activator inhibitor-1 (PAI-1) inhibitor tiplaxtinin was purchased from AdooQ BioScience (Irvine, CA, USA). The γ-secretase inhibitor DAPT was purchased from Sigma-Aldrich (St. Louis, MO, USA). The AKT inhibitors LY-294002 and BKM-120 were purchased from Wako Pure Chemical and AdooQ BioScience, respectively.

2.3. Animals

Six-week-old male severe combined immunodeficient (SCID) mice were obtained from CLEA Japan (Tokyo, Japan). Mice were maintained under specific pathogen-free conditions throughout the study. All experiments were performed in accordance with the guidelines established by the Tokushima University Committee on Animal Care and Use. At the end of each experiment, the mice were anesthetized with isoflurane and euthanized humanely by cutting the subclavian artery. All experimental protocols were reviewed and approved by the animal research committee of Tokushima University, Japan.

2.4. In vivo subcutaneous xenograft model of human lung cancer cells

For subcutaneous implantation, each SCID mouse had the skin of its bilateral flanks shaved and sterilized using 70% ethanol. Various numbers of A549 cells ($1–10 \times 10^4$ cells per mouse) or SBC-5 cells ($1–2.5 \times 10^5$ cells per mouse) with or without either human monocytes (2×10^5 cells per mouse) or fibrocytes (2×10^5 cells per mouse) were injected subcutaneously into the flank of the mice. The tumor volume was calculated using the formula, length × width squared × 0.5. The frequency of cancer-initiating cells (CICs) at four weeks after inoculation was calculated using the ELDA software program [7]. The mice were killed humanely under anesthesia when the tumor volume exceeded 1000 mm^3. To examine the effect of LY-294002 on the tumorigenic capacity of A549 cells, A549 cells were pretreated with LY-294002 (10 μM) for 2 h before subcutaneous injection.

2.5. Isolation of human monocytes and fibrocytes

Human mononuclear cells and fibrocytes were isolated from the peripheral blood of healthy volunteers according to previously published methods [8]. Greater than 90% of cells prepared in this methods were consisted of fibrocytes as determined by the expression of CD45, collagen I, and CXCR4 [8]. $CD14^+$ monocytes were purified from mononuclear cells by positive selection using anti-CD14 antibody and an Auto MACS cell separator (Miltenyi Biotech, Surrey, UK). Informed consent was obtained from all volunteers, and the protocol was approved by the Institutional Review Board (IRB) of Tokushima University Hospital (IRB approval number: 1586).

2.6. Preparation of conditioned medium from human monocytes and fibrocytes

Human monocytes or fibrocytes were suspended at 2.5×10^5 cells ml^{-1} in DMEM containing 10% FBS. Two milliliters of cell suspension were seeded into each well of a 6-well plate and cultured for 24 h. The attached cells were washed three times with PBS, and the medium was replaced with DMEM containing 0.1% FBS. After 48 h, the conditioned medium (CM) was harvested. CM was filtered through a 0.22-μm filter (EMD Millipore, Darmstadt, Germany) and stored at −80 °C for further analyses.

2.7. Sphere-forming assay

Cultured cells were trypsinized and passed through a 40-μm cell strainer (Corning, New York, NY, USA) to form a single-cell suspension. The cells were washed with PBS and suspended at 2×10^3 cells ml^{-1} (A549), 5×10^2 cells ml^{-1} (SBC-5), or 2×10^4 cells ml^{-1} (human fibrocytes) in DMEM containing 0.1% FBS. The tumor cell suspension (100 μl) was plated into each well of a 96-well ultra-low-attachment plate (Corning). The same amount of cell suspension for fibrocytes or CM of either monocytes or fibrocytes was added to each well and cultured for 14 days (A549) or 21 days (SBC-5). Tumor spheres (>50 μm) were counted under a microscope BZ-9000 (Keyence, Osaka, Japan). The sphere-forming efficiency (%) was calculated as the number of spheres divided by the number of single cells seeded [9].

2.8. Quantitative reverse transcription polymerase chain reaction

Reverse transcription polymerase chain reaction (RT-PCR) was performed according to a previously published method [5]. Human glyceraldehyde-3-phosphate dehydrogenase mRNA was used as a loading control. The specific PCR primer pairs used for each gene are shown in Supplementary Table 1.

2.9. MTT assay

Cells were plated into a 96-well plate at density of 5×10^3 cells per well and allowed to adhere for 24 h in DMEM containing 10% FBS. The cells were starved in DMEM containing 0.1% FBS for 24 h and then treated with serial concentrations of cisplatin, LY-294002, and BKM-120 for 48 h. After incubation, an MTT assay was performed according to a previously published method [5].

2.10. Membrane-based cytokine array

Experiments were performed using a Human XL Cytokine Array Kit (R&D Systems) according to the manufacture's instruction. Quantitative analyses were performed using the ImageJ plugin.

2.11. Detection of protein expression in cancer cells

Cells were seeded in 6-well plates and allowed to adhere for 24 h in RPMI 1640 containing 10% FBS. Cells were starved in serum-free DMEM for 24 h and pretreated with LY-294002 (10 μM), BKM-120 (10 μM), or vehicle for 2 h. Cells were then treated with OPN (1 μg/ml), CCL-18 (100 ng ml^{-1}), or CM from fibrocytes for the indicated durations. Whole-cell extracts from cancer cells were isolated using M-PER (Pierce, Rockford, IL, USA) containing phosphatase and protease inhibitor cocktails (Roche, Basel, Switzerland). The concentrations of proteins were determined using a TaKaRa BCA Protein Assay Kit (Takara Bio Inc., Shiga, Japan). Samples of 200 μg ml^{-1} of total proteins were used for an automated capillary western assay using Wes instruments (Protein Simple, San Jose, CA, USA) according to the manufacturer's instructions. Primary antibodies against phospho-Akt (4060) and Akt (9272) were purchased from Cell Signaling Technology (Beverly, MA, USA).

2.12. Clinical study population

We collected 58 consecutive cases of surgically resected lung cancer patients with stage IA-IIIA in 2012 at Tokushima University Hospital. We retrospectively analyzed their outcomes from the electronic medical records. Twenty-four of 48 adenocarcinoma cases were further analyzed CSC-related protein expression on cancer cell. The current study was approved by the IRB of Tokushima University Hospital (IRB approval number: 2471), and informed consent was obtained from all patients.

2.13. Immunohistochemical studies of the patient samples

Fibrocyte-like cells in the clinical specimens were identified using anti-CD45 and anti-fibroblast-specific protein 1 (FSP-1) antibody as previously described [5]. The patients were divided into two groups according to the receiver operating characteristic (ROC) analysis of the number of stromal fibrocyte-like cells (Supplementary Fig. 1A and Supplementary Table 2); fibrocytes-high, 15 patients with ≥12.6 fibrocyte-like cells per field on average; fibrocytes-low, 43 patients with <12.6 fibrocyte-like cells per field on average at ×400 magnification in the tumor stroma. Collagen deposition in the tumor tissues were analyzed using Azan stain, and the blue color area of the tumor was measured using ImageJ plugin. To detect the CSC-associated protein in lung cancer cells, a rabbit anti-sex determining region Y-box 2 (Sox-2) polyclonal antibody (1:150 dilution, NB110-37235; Novus Biologicals, Littleton, CO, USA), a rabbit anti-Nanog monoclonal antibody (1:100 dilution, ab109250; Abcam), and a rabbit anti-octamer-binding transcription factor 4 (Oct-4) polyclonal antibody (1:200 dilution, #2750; Cell Signaling Technology) were used. A human testis seminoma tissue slide was used as a positive control (Gene Tex, Irvine, CA, USA). A lung cancer tissue array (LC806) was purchased from US Biomax, Inc. (Rockville, MD, USA).

The sections were re-incubated with an anti-rabbit secondary antibody conjugated with peroxidase (ready to use; Nichirei, Tokyo, Japan). Immunoreactivity was detected using the 3,3′-diaminobenzidine Tetrahydrochloride (DAB) Liquid System (Nichirei), and samples were counterstained with hematoxylin. Immunohistochemical positivity was defined as tissue in which >10% of tumor cells were positive for DAB. Images were acquired using a microscope (BZ-9000; Keyence).

2.14. Statistical analyses

The data are shown as the mean ± standard error of the mean (SEM). Statistical analyses were performed using Student's *t*-test with or without Welch's correction, or the Mann-Whitney *U* test for unpaired samples, as appropriate. A one-way analysis of variance (ANOVA) followed by Tukey's multiple-comparison post-hoc test was used for comparisons among more than two groups. The overall survival (OS) and disease-free survival (DFS) was defined as the time from diagnosis of lung cancer to the date of death from any cause and the time from date of surgery to the date of recurrence of lung cancer or death from any cause, respectively. Patients who were alive at the time of analyses were censored at the last known date of follow-up. The survival was estimated using the Kaplan-Meier method, and the log-rank test was used to assess differences in the survival distributions between groups. Multivariate analyses were performed with the Cox proportional hazards model to identify variables that were independently predictive of outcome. Factors with *p*-values <0.05 on univariate analyses were entered as candidate variables. Resulting *p*-values of <0.05 were considered to be significant. Statistical analyses were performed using the GraphPad PRISM software program (5.01; GraphPad Software, Inc., La Jolla, CA, USA) and R software (3.1.1; The R Foundation for Statistical Computing).

3. Results

3.1. The accumulation of fibrocytes in human lung cancer tissue

Initially, to determine whether or not fibrocytes were involved in lung cancer progression in clinical settings, we carried out immunohistochemical studies with surgically resected samples from lung cancer patients. Fibrocytes in the tissue section are usually identified with the expression of a marker of fibroblasts such as collagen production together with the expression of CD34 and/or CD45 [4]. However, these approaches may include some population of fibroblasts and macrophages. Therefore, we used the term of fibrocyte-like cells in clinical settings and identified fibrocyte-like cells with both CD45 and FSP-1 expressed cells as previously described [5]. The patients were divided into two groups according to the ROC analysis of the number of stromal fibrocyte-like cells (See Material and Methods, and Supplementary Fig. 1A) and the clinicopathological features were summarized in Supplementary Table 2. We found that the survival of patients in the fibrocytes-high group was significantly worse than in the fibrocytes-low group (Fig. 1A and B). As the interaction between extracellular matrix (ECM) and tumor cells regulates cancer progression [10], and as fibrocytes are known to produce collagen [4] we analyzed collagen deposition, which is the main component of the ECM, in tissue samples from lung adenocarcinoma patients. However, the correlation between collagen deposition in the tumor and number of stromal fibrocyte-like cells was not found (Supplementary Fig 1B). In the univariate analysis, clinical stage, and gender were also significantly associated with poor prognosis (Table 1). Based on the results of univariate analysis, variables of the number of stromal fibrocytes, clinical stage, and gender were applied into multivariate Cox proportional hazard regression model, and all the variables were independent poor prognostic factors in resectable lung cancer patients (Table 1). These results indicated that proinflammatory properties rather than tissue remodeling properties of fibrocytes were involved in cancer progression in the tumor microenvironment of lung cancer.

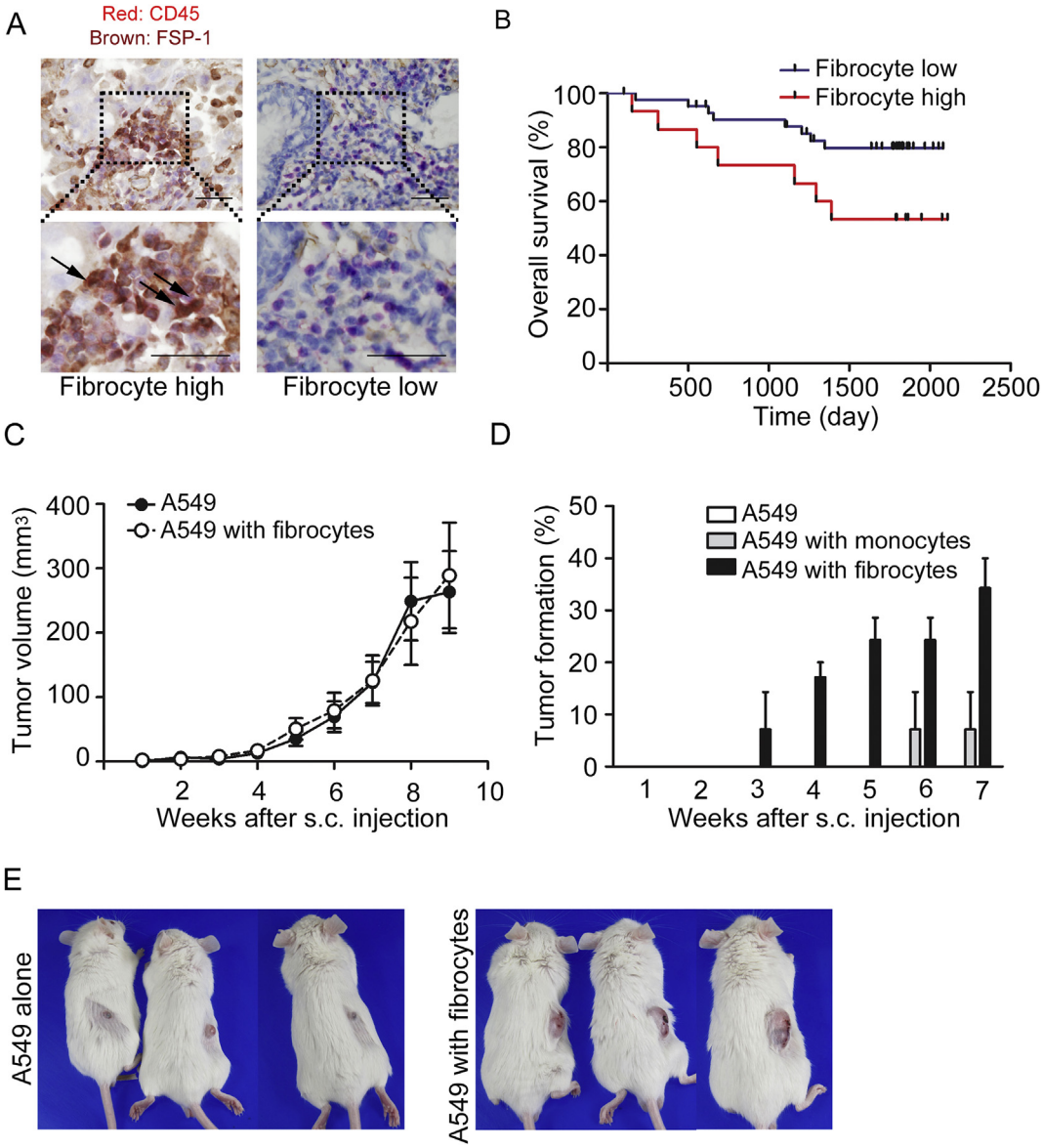

Fig. 1. Fibrocytes promote the tumorigenic ability of lung cancer cells *in vivo*. **A,** Fibrocyte-like cells were identified using double immunohistochemistry, and representative images of staining for CD45 (red) and/or FSP-1 (brown) in the section from resectable lung adenocarcinoma patients are shown. The arrow indicates double-positive cells. Scale bar upper panels, 200 μm; scale bar lower panels, 50 μm. **B,** Kaplan-Meier estimates of the probability of a OS in the fibrocytes-high group (n = 15, red line) and fibrocytes-low group (n = 43, blue line) were compared. The median OS was not reached in either group. There was a significant difference in the OS between the two groups (hazard ratio, 3.36; 95% confidence interval, 1.03–10.91; $P = 0.044$). The P value was calculated using the log-rank test. **C,** A549 cells were implanted into SCID mice to form subcutaneous xenografts. Tumor volume after subcutaneous injection of A549 (1×10^5 cells/mouse) with or without fibrocytes is presented ($n = 5$ per group). **D,** The tumor formation rate after subcutaneous co-injection of A549 (1×10^4 cells/mouse) with or without either human monocytes or fibrocytes was evaluated ($n = 5$–7). The experiment was performed in duplicate. **E,** Gross appearances of the tumors in mice 11 weeks after subcutaneous injection of A549 cells (5×10^4 cells/mouse) alone (upper) and with fibrocytes (lower). All data are shown as the means ± SEM. (For interpretation of the references to color in this figure legend, the reader is referred to the Web version of this article.)

3.2. Contribution of fibrocytes to tumorigenesis of lung cancer cells in vivo

To further assess whether or not fibrocytes enhanced tumor growth of lung cancer cells, we isolated human fibrocytes from peripheral blood of healthy volunteers, and conducted an *in vivo* study by subcutaneously injecting human lung adenocarcinoma A549 cells (1×10^5 cells) with or without human fibrocytes (2×10^5 cells) into SCID mice. Human fibrocytes were first confirmed to be alive and resided in the tumor for 72 h after inoculation into tumor-bearing mice (Supplementary Fig. 1C). Four weeks after the injection, all mice developed subcutaneous tumors (Table 2); however, no marked differences were seen in the tumor growth between two groups (Fig. 1C). We next assessed whether or not fibrocytes contribute to the tumor initiation of lung cancer cells. When a small number of A549 cells (1×10^4 or 5×10^4 cells) was injected with or without either human fibrocytes (2×10^5 cells) or monocytes (2×10^5 cells) into SCID mice, A549 cells co-injected with fibrocytes formed subcutaneous tumors earlier than those co-injected with PBS or monocytes (Fig. 1D) and formed a larger tumor at the endpoint (Fig. 1E). The frequency of CICs, which display the properties of CSCs, at four weeks after the inoculation of A549 cells was significantly enhanced by co-injection with fibrocytes compared with co-injection with PBS or monocytes (Table 2), suggesting that the fibrocytes were able to initiate tumor formation of A549 cells via paracrine factors and/or cell-cell contact. Similar

Table 1
Univariate and multivariate analyses for death of lung cancer patients.

Variables	Univariate analysis		Multivariate analysis	
	HR (95% CI)	*p*-value	HR (95% CI)	*p*-value
Age				
70 > vs. <70	1.13 (0.41–3.15)	0.809		
Gender				
Male vs. Female	3.48 (1.25–9.69)	0.017	4.88 (1.03–23.08)	0.046
Clinical stage				
II, III vs. I	11.09 (3.17–38.82)	0.001	3.49 (1.19–10.26)	0.023
Smoking status				
Smoker vs. Never-smoked	1.40 (0.62–3.19)	0.417		
Number of fibrocytes				
high vs. low	3.36 (1.03–10.91)	0.044	2.90 (1.00–8.39)	0.050

HR, hazard ratio; CI, confidence interval.
Overall survival was estimated using the Kaplan-Meier method, and the log-rank test was used to assess differences in the survival distributions between variables.

Table 2
The frequency of CICs in lung cancer cells *in vivo*.

A549	Tumor formation			1/CIC frequency (95% CI)	*P* value	
	1×10^5 cells	5×10^4 cells	1×10^4 cells			
Control	5/5	0/11	0/11	Inf (Inf–220313)	0.248[a]	
With monocytes		1/12	0/12	694701 (4910248–98286)	0.030[c]	0.003[b]
With fibrocytes	5/5	4/12	2/12	100259 (226975–44286)		
SBC-5		**5×10^5 cells**	**2.5×10^5 cells**	**1/CIC frequency (95% CI)**	***P* value**	
Control		0/5	0/5	Inf (Inf–1251781)	0.003[b]	
With fibrocytes		3/5	2/5	522460 (1287716–211975)		

CI, confidence interval.
The frequencies of CICs and *P* values were calculated using ELDA software program.
[a] Compared with control and monocyte.
[b] Compared with control and fibrocyte.
[c] Compared with monocyte and fibrocyte.

results were obtained using the human small cell lung cancer cell line SBC-5 (Table 2).

3.3. Enhancement of the sphere-forming ability of lung cancer cells by fibrocytes

Since *in vivo* results suggested the ability of fibrocytes to promote CSC properties of lung cancer cells, we next assessed the sphere-forming ability of lung cancer cells, which is one of the functional methods for evaluating the properties of CSCs *in vitro* [11]. A549 and SBC-5 cells were cultured with either CM from monocytes or fibrocytes in ultra-low-attachment plates. Although these cells rarely formed tumor spheres when cultured with CM from monocytes, the sphere-forming efficiency was significantly increased when these cells were cultured with CM from fibrocytes (Fig. 2A). Similar effect was observed using fibrocytes from lung cancer patients (Supplementary Fig 2A). These results suggested that paracrine factor from fibrocytes might promote CSC-like properties of lung cancer cells.

To confirm the CSC-like properties of sphere-forming cells induced by fibrocytes, the expression of the stemness-associated genes *Oct-4*, *Sox-2*, and *Nanog* in sphere-forming cells was assessed. The mRNA expression of these genes in sphere-forming cells was significantly upregulated compared with that in parental cells (Fig. 2B). Drug resistance is also an important property of CSCs [11]. Sphere-forming cells were more resistant to cisplatin treatment than in parental cells (Supplementary Fig. 2B). Furthermore, the mRNA expression of *ABCG2* and *ABCB1* genes, which are associated with resistance to multiple drugs, was significantly higher in sphere-forming cells than in parental cells (Supplementary Fig. 2C). Sphere-forming cells displayed a significantly greater cancer-initiating capacity than parental cells (Fig. 2C and Supplementary Table 3). These results further supported the notion that soluble factors derived from fibrocytes induced CSC-like properties of lung cancer cells.

3.4. Enhancement of CSC-like properties of lung cancer by paracrine factors from fibrocytes

To identify the factors secreted by fibrocytes that enhanced the CSC-like phenotype of lung cancer cells, we compared the cytokine and chemokine profiles of fibrocytes with that of monocytes using a membrane-based protein array. Five secreted proteins were identified as more than five-fold increased in the CM of fibrocytes compared with that of monocytes from two different donors (Fig. 3A and Supplementary Table 4). An oligonucleotide microarray analysis was also performed, and 10 putative secreted genes were identified that were significantly upregulated (more than 200-fold) in fibrocytes compared with monocytes (Supplementary Table 5).

Based on these results, we focused on CH3L1, GDF-15, PAI-1, OPN, MMP-9, CCL-2, CCL-7, and CCL-18 for future examinations. The respective functions of these proteins in the sphere-forming ability of lung cancer cells were assessed using neutralizing antibodies or specific inhibitors. Although the results varied among fibrocytes donors, the neutralizing antibody for OPN and CCL-18 as well as PAI-1 inhibitor reduced the fibrocyte-mediated spheroid formation

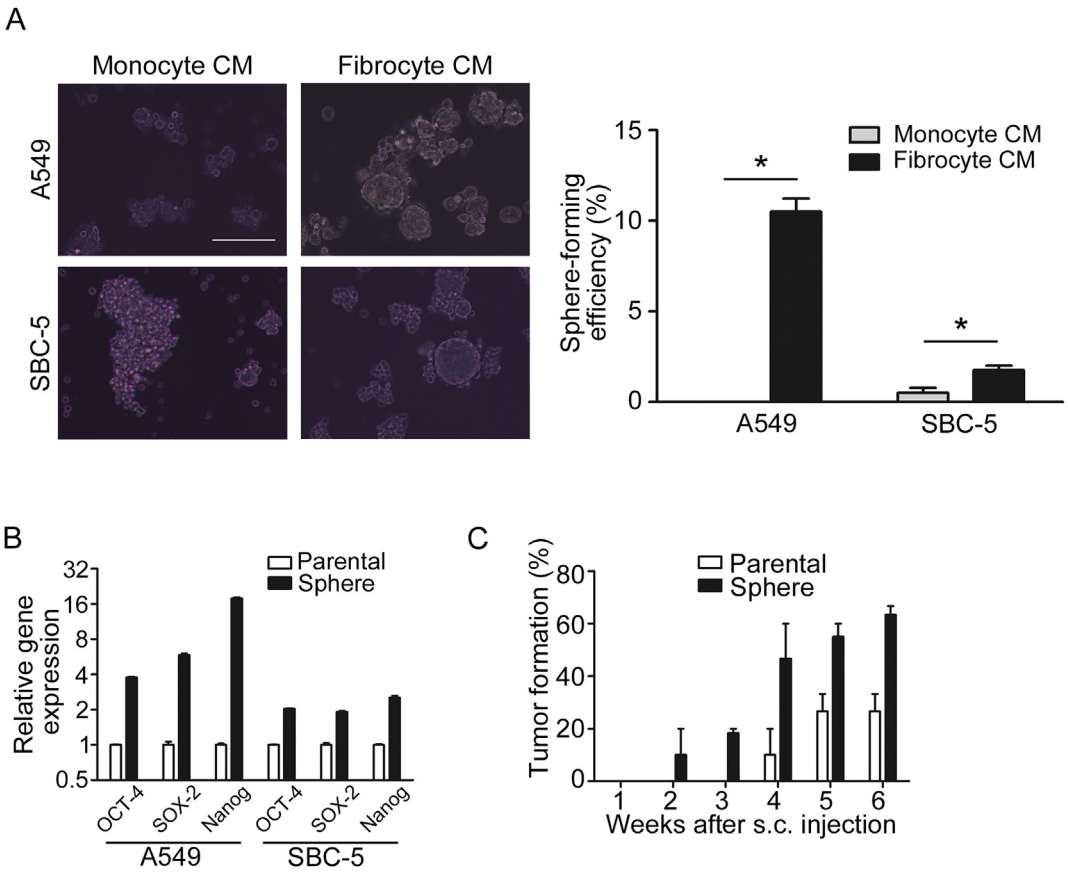

Fig. 2. Soluble factor derived from fibrocytes induced the CSC-like phenotype in lung cancer cells *in vitro*. **A,** A549 and SBC-5 cells were cultured with CM from either monocytes or fibrocytes in ultra-low-attachment plates. A representative image of tumor spheres is presented at left panel. Scale bar, 200 μm. The number of spheres with a diameter greater than 50 μm was quantified on day 14 (A549) or day 21 (SBC-5). The quantitative analysis of sphere forming efficiency is shown in the right panel ($n = 4$). The experiment was performed in triplicate. $^*P < 0.05$, and P values were calculated using Student's t-test with Welch's correction. **B,** A549 or SBC-5 cells were treated with CM from fibrocytes under ultra-low-attachment conditions for seven days, and the mRNA expression of CSC-associated genes in parental and sphere-forming cells was detected with a quantitative real-time PCR analysis ($n = 3$). The experiment was performed in triplicate. $P < 0.05$, and P values were calculated using Student's t-test. **C,** Parental A549 cells or sphere-forming cells (5×10^4 cells/mouse) were subcutaneously inoculated into SCID mice. The tumor formation rate after subcutaneous injection was evaluated ($n = 5$ per group). The experiment was performed in duplicate. All data are shown as the means ± SEM.

of A549 cells (Fig. 3B), while neutralizing antibodies for other proteins did not inhibit the fibrocyte-mediated spheroid formation (Supplementary Fig. 3A). An additive effect of anti-OPN and anti-CCL-18 antibody on fibrocyte-mediated spheroid formation of A549 cells was not observed (Supplementary Fig. 3B), suggesting that these two proteins might share the intracellular signaling pathways. γ-Secretase is involved in OPN-CD44 signaling through the release of CD44 C-terminal intracellular domain similar to Notch signaling [12]. The γ-secretase inhibitor DAPT inhibited the fibrocyte-enhanced sphere formation of A549 cells, further supporting the involvement of OPN in the fibrocyte-mediated sphere-forming ability of A549 cells (Fig. 3B). However, recombinant OPN, CCL-18, and PAI-1 did not enhance the sphere formation of lung cancer cells (Supplementary Fig. 3C), even with combination treatment, suggesting that although these proteins were secreted by fibrocytes, other unidentified factors may modify their ultimate effect on spheroid formation [13,14].

3.5. Importance of the PIK3K/AKT pathway for fibrocyte-mediated CSC-like properties of lung cancer cells

OPN, CCL-18, and PAI-1 are reported to play important roles in the tumor progression via the activation of the PI3/AKT pathway [12,15–18], so we focused on the AKT pathway of lung cancer cells. CM from fibrocytes as well as recombinant OPN and CCL-18 increased the phosphorylation of AKT protein of lung cancer cells (Fig. 4A), and these effects were inhibited by the AKT inhibitors LY-294002 and BKM-120 (Fig. 4B and Supplementary Fig. 4A). Furthermore, LY-294002 and BKM-120 significantly suppressed the fibrocytes-mediated sphere-forming capacity of lung cancer cells at a dose that did not affect the proliferation of lung cancer cells *in vitro* (Fig. 4C and Supplementary Fig. 4B and 4C).

To validate the importance of the PI3K/AKT pathway in fibrocyte-mediated tumorigenesis *in vivo*, A549 cells were pretreated with LY-294002 prior to their subcutaneous injection into SCID mice. Although the pretreatment of LY-294002 itself did not affect the subcutaneous tumor growth of A549 cells (1×10^5 cells/mouse), co-injection of fibrocytes with a decreased number of A549 cells (1×10^4 cells/mouse) pretreated with LY-294002 significantly reduced the tumor formation and frequency of CICs (Fig. 4D and E, and Table 3). These results suggested that the PI3K/AKT pathway was strongly associated with the fibrocyte-mediated acquisition of CSC-like properties of lung cancer cells.

3.6. Association of the number of tumor-infiltrated fibrocytes with the CSC-like phenotype of lung cancer cells in clinical specimens

Finally, to assess the interaction between fibrocytes and the

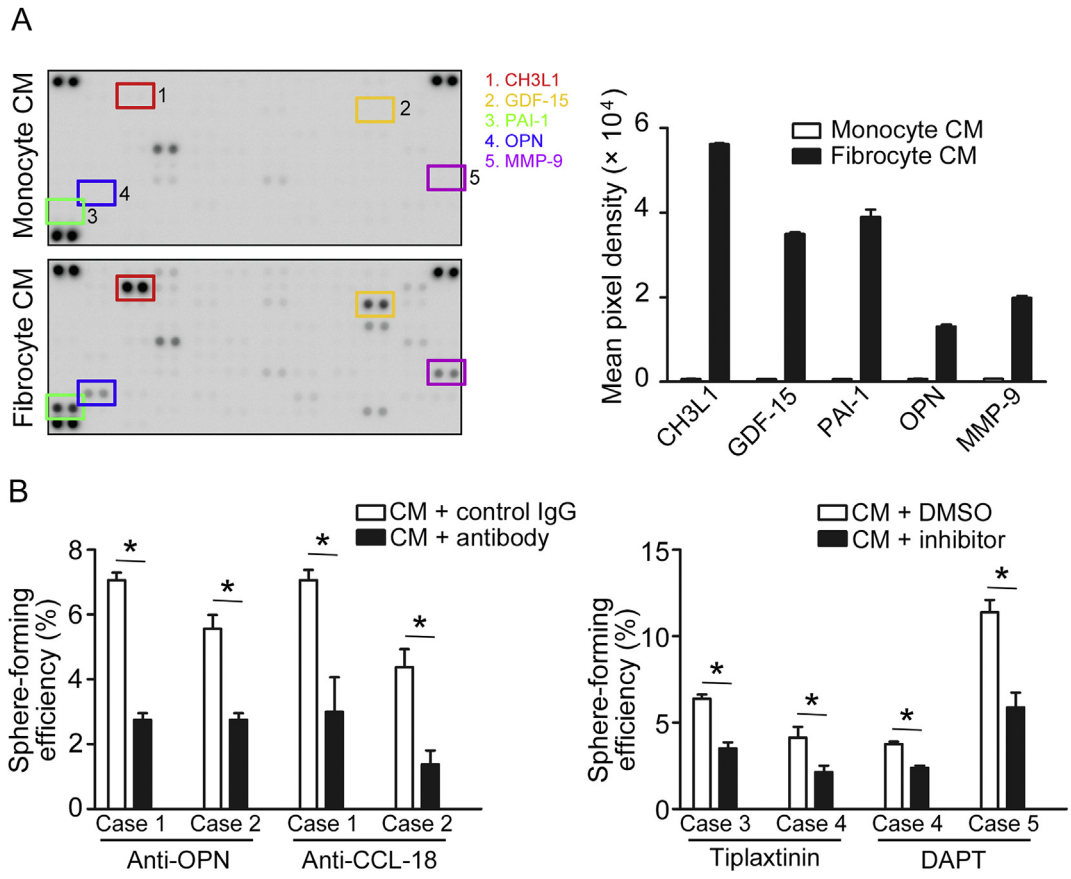

Fig. 3. Paracrine factors from fibrocytes enhance the sphere-forming ability of lung cancer cells. **A.** Membrane-based protein arrays of CM from fibrocytes and monocytes were performed for two different donors. The representative image of the membrane is shown in the left panel. The mean pixel density of indicated cytokines from monocyte and fibrocyte was calculated using the Image J software program (right panel). **B,** The inhibitory effect of neutralizing antibodies for OPN (10 μg/ml) and CCL-18 (5 μg/ml) and the specific inhibitor to PAI-1 (tiplaxtinin, 0.5 μM) and γ-secretase (DAPT 5 μM) on the fibrocyte-inducing sphere-forming ability of A549 cells was evaluated ($n = 4$). The experiment was performed in triplicate using CM from two different donors. $^{*}P < 0.05$, and P values were calculated using Student's t-test. All data are shown as the means ± SEM.

CSC-like phenotype of lung cancer cells in the clinical setting, we carried out immunohistochemical studies with surgically resected samples from lung cancer patients. Sox-2 and Nanog protein expression were reported to be an independent poor prognostic factor in resectable lung adenocarcinoma patients [19,20], so we investigated the expression of these proteins in our lung adenocarcinoma samples.

Among 24 adenocarcinoma tissues, 10 had positive staining for Sox-2, with a positive rate of 41.6%, and 14 cases had positive staining for Nanog, with a positive rate of 58.3%. These results were consistent with previous reports [19,20]. Furthermore, the number of fibrocyte-like cells was significantly higher in the tumor-stroma of Sox-2 and Nanog-positive cases than in negative cases (Fig. 5A). Unlike previous reports, the Sox-2 and Nanog expression was not associated with the DFS in our study (date not shown). Because Oct-4-positive cancer cells were rarely observed in early-stage lung adenocarcinoma samples, we further analyzed the Oct-4 expression using a lung cancer tissue array, which contained a variety of lung cancer sections from various stages. Twenty-nine cases of 72 lung cancer tissues were positive for Oct-4 staining, with a positive rate of 40.3%. In addition, the number of fibrocyte-like cells was significantly higher in the tumor stroma of Oct-4-positive cases than that in Oct-4-negative cases (Fig. 5B). These findings support our pre-clinical data suggesting that fibrocytes might be a pivotal cell that regulates the CSC-like fate of lung cancer cells in the CSC niches.

4. Discussion

Fibrocytes are differentiated from bone-marrow derived monocytes and share the inflammatory features of macrophages and tissue remodeling properties of fibroblasts [21]. Based on their inflammatory and fibrogenic abilities, fibrocytes were previously reported to be involved in the pathogenesis of various fibrotic diseases, such as asthma and interstitial pulmonary fibrosis [4,22]. In the tumor microenvironment, however, only a few studies have reported their immunosuppressive role and tumor-promoting ability [23–25], and the role of fibrocytes in the tumor microenvironment is not fully elucidated. To our knowledge, we have demonstrated for the first time their role in CSC niches.

In CSC niches, CAFs are reported to be the most prominent cells [26]. Fibrocytes are a distinct cell population from CAFs in that they express hematopoietic cell markers CD34 and CD45, and chemokine receptor CXCR4 [21]. However, completely distinguishing these cell types in the tissue seems difficult for several reasons. First, CAFs are a heterogeneous cell-subset and largely defined based on the expression of α-smooth muscle actin, fibroblast activation protein, and platelet-derived growth factor receptor-β [27]. These markers are not specific to CAFs and can also be expressed by fibrocytes [4,28]. Second, some studies have shown that bone marrow-derived precursor cells contribute to the CAF population in addition to local fibroblasts [29], suggesting that fibrocytes may have been included in the heterogeneous CAF subsets in previous studies.

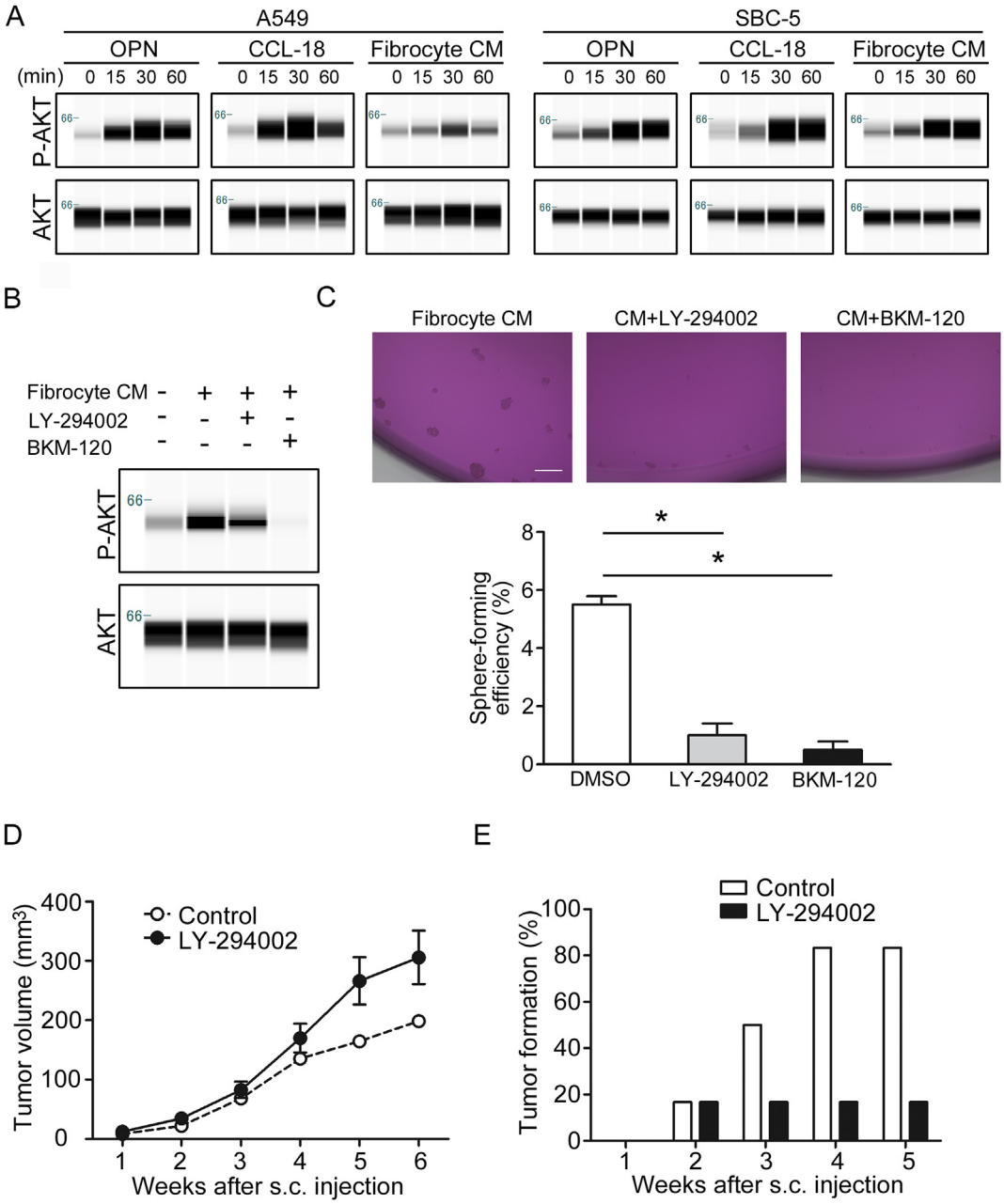

Fig. 4. Fibrocytes enhance the CSC-like properties of lung cancer cells via the PIK3K/AKT pathway. **A,** A549 and SBC-5 cells were cultured with OPN (1 μg/ml), CCL-18 (100 ng ml^{-1}), or CM from fibrocytes for the indicated duration. The phosphorylation of AKT was detected by an automated capillary western assay. Total AKT was used as the loading control. **B,** A549 cells were pretreated with the AKT inhibitors LY-294002 (20 μM) or BKM-120 (10 μM), or vehicle for 2 h. Cells were then treated with CM from fibrocytes for 30 min. The phosphorylation of AKT was detected by an automated capillary western assay. Total AKT was used as loading control. **C,** A549 cells were cultured in CM from fibrocytes with or without either LY-294002 (1 μM) or BKM-120 (250 nM) on an ultra-low-attachment palate. The representative image of tumor cells in each well is shown in the upper panel. Scale bar, 200 μm. The number of spheres with a diameter greater than 50 μm was quantified on day 14, and the sphere-forming efficiency is shown in the lower panel ($n = 4$). The experiment was performed in triplicate. $^{*}P < 0.05$, and P values were calculated using a one-way ANOVA followed by Tukey's post hoc test. **D,** A549 cells were pretreated with DMSO or LY-294002 (10 μM) for 2 h. A549 cells (1×10^5 cells/mouse) were then subcutaneously injected into the flank of SCID mice. The tumor volumes after subcutaneous injection are shown. ($n = 6$ per group). **E,** A549 cells were pretreated with DMSO or LY-294002 (10 μM) for 2 h. A549 cells (1×10^4 cells/mouse) were then subcutaneously co-injected with human fibrocytes into the flank of SCID mice. The tumor formation rate after subcutaneous injection is shown ($n = 6$ per group). All data are shown as the means ± SEM.

TAMs are also a key component of CSC niches [30]. In human clinical specimens, macrophages can be identified from cancer cells using CD68 or myeloid cell surface markers, CD14, HLA-DR, CD312, CD115, and CD16. TAMs are further phenotyped using M2 subset-specific markers, including CD163, CD204, and CD301, and the tolerogenic macrophage-expressed scavenger receptor CD206 [31]. These markers are not static and can be changed by the tumor microenvironment [31]. Both fibrocytes and TAMs are differentiated from bone marrow-derived $CD14^{+}$ precursor cells and express common cell surface markers, including CD11b, CD68, CD163, and CD206 [1]. Furthermore, on stimulation with GM-CSF or M-CSF, the expression of collagen on fibrocytes was found to be downregulated, and fibrocytes were differentiated into macrophages [32]. These findings suggested that fibrocytes can differentiate into a TAM subset in response to changes in the tumor microenvironment in CSC niches and might have made up a portion

Table 3
The frequency of CICs in A549 cells *in vivo*.

A549		Tumor formation			1/CIC frequency (95% CI)	*P* value
		1×10^5 cells	5×10^4 cells	1×10^4 cells		
With PBS	Vehicle	6/6	1/5		63771 (137828–29507)	1.000
	LY-294002	6/6	1/5		63771 (137828–29507)	
With fibrocyte	Vehicle			5/6	5582 (15150–2057)	0.016
	LY-294002			1/6	54849 (390430–7706)	

CI, confidence interval.
The frequencies of CICs and *P* values were calculated using ELDA software program.

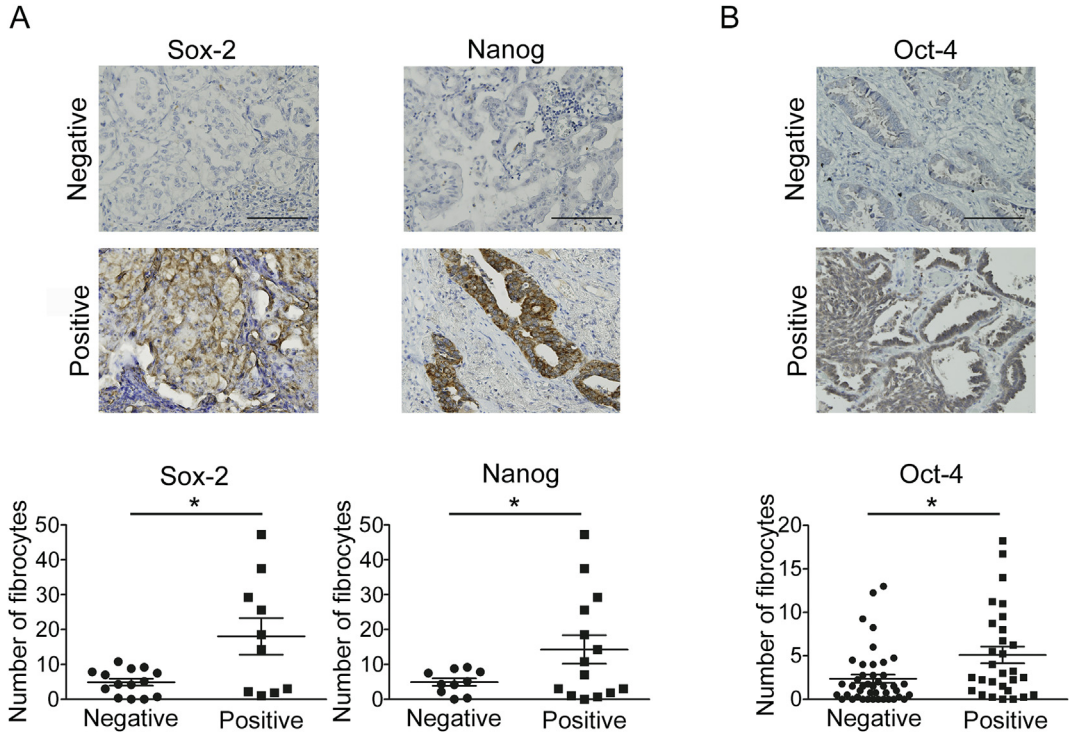

Fig. 5. The number of tumor-infiltrated fibrocyte-like cells is associated with the CSC-like phenotype of lung cancer cells in clinical specimens. **A,** The representative images of negative or positive staining for Sox-2 or Nanog in tumor cells are shown in the upper panel. Scale bar, 200 μm. Lung adenocarcinoma patients were divided into two groups according to the expression of Sox-2 or Nanog in the tumor cells, and the number of stromal fibrocyte-like cells was compared between the two groups ($n = 24$, lower panel). $^*P < 0.05$, and *P* values were calculated using Student's *t*-test with Welch's correction. **B,** The expression of Oct-4 in tumor cells and the number of fibrocyte-like cells in tumor stroma was assessed using a lung cancer tissue array. The representative images of negative or positive staining for Oct-4 in tumor cells are shown in the upper panel. Scale bar, 200 μm. The number of stromal fibrocyte-like cells in the Oct-4-negative group and Oct-4-positive group were compared ($n = 72$, lower panel). $^*P < 0.05$, and *P* values were calculated using Student's *t*-test with Welch's correction. All data are shown as the means ± SEM.

of M2 macrophage or TAM subsets in previous studies.

A previous study showed that MDSCs isolated from human breast cancer enhanced the CSC-like properties of breast cancer cells by activating STAT3 and NOTCH [33]. MDSCs comprise a heterogeneous population of bone marrow-derived cells that include diverse states of differentiation, from early myeloid to a more granulocytic or monocytic phenotype [34]. Recently, $CCR2^+$ MDSCs subset were found to be differentiated into fibrocytes and promoted tumor metastasis [35]. Furthermore, circulating fibrocytes were reported to have features of an MDSC subset, such as immune evasion, and contributed to tumor progression [24]. Thus, both MDSCs and fibrocytes include heterogeneous populations and have common features and origins. In addition, the molecular markers that distinguish these cells have not clearly been established. Therefore, further studies to investigate the MDSC-like features and molecular markers of the MDSC subset among fibrocytes in CSC niches are needed.

The present study demonstrated that fibrocytes regulate the CSC-like properties of lung cancer cells by providing OPN, CCL-18, and PAI-1. OPN is a small integrin-binding ligand N-linked glycoprotein and is produced by both CAFs and TAMs [13,26,36]. OPN secreted from CAFs increased the CSC population of colorectal cancer cells by activating the PI3K/AKT pathway [37]. Furthermore, OPN produced from TAMs facilitated the tumorigenicity of CD44-positive colorectal cancer cells via c-jun-NH2-kinase signaling [38]. Thus, OPN appears to be one of the most important factors derived from host cells in the CSC niche. CCL-18 is a chemokine predominantly produced by TAMs and highly expressed in lung with several pathologies, including malignancy and fibrosis [39]. CCL-18 enhanced metastasis by inducing epithelial to mesenchymal transition (EMT) in lung and breast cancer via the activation of the AKT/GSK3β pathway [16,39–41]. EMT endows CSC-like

properties in mammary epithelial cells [42]. Thus, CCL-18 is also a niche-cell-derived factor that promotes a CSC-like fate. These findings suggest that fibrocytes may be a novel cell population that facilitate the induction of CSC-like properties in lung cancer by producing OPN and CCL-18 in CSC niches.

PAI-1 is a secreted protein that inhibits urokinase-type plasminogen activator (u-PA) and plays an important role in the plasminogen-plasmin system [43]. The proteolytic enzyme plasmin is activated by u-PA and facilitates tumor migration and invasion by the degradation of the ECM and activation of latent growth factors [14]. Earlier studies have therefore suggested that PAI-1 might suppress tumor progression. However, a high PAI-1 expression of tumor was found to be associated with a poor prognosis in many types of cancer. Recent studies have demonstrated that PAI-1 inhibited cell apoptosis by inactivating caspase-3 or upregulating the PI3K/AKT and Jak/STAT pathways [44]. Furthermore, PAI-1 induced the expression of EMT marker by activating the AKT and ERK1/2 pathways in lung cancer [18]. Taken together, these findings suggest that PAI-1 might promote tumor progression rather than tumor inhibition through an anti-proteolytic effect in the tumor microenvironment and may be a niche-cell-derived factor that regulates the CSC-like properties of cancer cells.

In summary, we identified fibrocytes as a novel cell population regulating the CSC-like properties of lung cancer by activating the AKT pathway thorough secreted factors, including OPN, CCL-18, and PAI-1. Although targeting the AKT pathway may provide a therapeutic strategy against CSCs, a further understanding of the CSC niche factors that regulate both CSC-like phenotype of lung cancer cells and recruitment of fibrocytes into CSC niche might help to develop a successful treatment strategy targeting CSCs.

Conflicts of interest

The authors declare that we have no conflict of interest.

Acknowledgement

We thank Drs. M. Tanimoto and K. Kiura (Okayama University, Okayama, Japan) for providing the cell line and Dr. M. Miyasaka (Osaka University, Japan) for providing TM-β1. We also thank our colleagues at Tokushima University, especially T. Oka for her technical assistance with primary cell isolation, Megumi Kume and Yuuki Morimoto for their technical assistance with preparing and staining thin sections of patients, and the members of the Nishioka lab for their technical advice and fruitful discussions.

This work was supported by the Japan Society for the Promotion of Science (JSPS) KAKENHI (Grant Number JP16K19456 and JP16H05309), Japan Agency for Medical Research and Development (AMED), and the Ministry of Health, Labour and Welfare of Japan. This work is a result of collaborative research with Taiho Pharmaceutical, Inc. (Tokyo, Japan).

Appendix A. Supplementary data

Supplementary data related to this article can be found at https://doi.org/10.1016/j.canlet.2018.02.016.

References

[1] D.F. Quail, J. a Joyce, Microenvironmental regulation of tumor progression and metastasis, Nat. Med. 19 (2013) 1423–1437, https://doi.org/10.1038/nm.3394.
[2] A. Kreso, J.E. Dick, Evolution of the cancer stem cell model, Cell Stem Cell. 14 (2014) 275–291, https://doi.org/10.1016/j.stem.2014.02.006.
[3] V. Plaks, N. Kong, Z. Werb, The cancer stem cell niche: how essential is the niche in regulating stemness of tumor cells? Cell Stem Cell. 16 (2015) 225–238, https://doi.org/10.1016/j.stem.2015.02.015.
[4] R. a Reilkoff, R. Bucala, E.L. Herzog, Fibrocytes: emerging effector cells in chronic inflammation, Nat. Rev. Immunol. 11 (2011) 427–435, https://doi.org/10.1038/nri2990.
[5] A. Mitsuhashi, H. Goto, A. Saijo, V.T. Trung, Y. Aono, H. Ogino, T. Kuramoto, S. Tabata, H. Uehara, K. Izumi, M. Yoshida, H. Kobayashi, H. Takahashi, M. Gotoh, S. Kakiuchi, M. Hanibuchi, S. Yano, H. Yokomise, S. Sakiyama, Y. Nishioka, Fibrocyte-like cells mediate acquired resistance to anti-angiogenic therapy with bevacizumab, Nat. Commun. 6 (2015) 1–15, https://doi.org/10.1038/ncomms9792.
[6] T. Kuramoto, H. Goto, A. Mitsuhashi, S. Tabata, H. Ogawa, H. Uehara, A. Saijo, S. Kakiuchi, Y. Maekawa, K. Yasutomo, M. Hanibuchi, S.-I. Akiyama, S. Sone, Y. Nishioka, Dll4-Fc, an inhibitor of Dll4-notch signaling, suppresses liver metastasis of small cell lung cancer cells through the downregulation of the NF-κB activity, Mol. Canc. Therapeut. 11 (2012) 2578–2587, https://doi.org/10.1158/1535-7163.MCT-12-0640.
[7] Y. Hu, G.K. Smyth, ELDA: extreme limiting dilution analysis for comparing depleted and enriched populations in stem cell and other assays, J. Immunol. Meth. 347 (2009) 70–78, https://doi.org/10.1016/j.jim.2009.06.008.
[8] R.J. Phillips, M.D. Burdick, K. Hong, M.A. Lutz, L.A. Murray, Y.Y. Xue, J.A. Belperio, M.P. Keane, R.M. Strieter, Circulating fibrocytes traffic to the lungs in response to CXCL12 and mediate fibrosis, J. Clin. Invest. 114 (2004) 438–446, https://doi.org/10.1172/JCI200420997.
[9] P. Zhu, M. Davis, A.J. Blackwelder, N. Bachman, B. Liu, S. Edgerton, L.L. Williams, A.D. Thor, X. Yang, Metformin selectively targets tumor-initiating cells in ErbB2-overexpressing breast cancer models, Canc. Prev. Res. 7 (2014) 199–210, https://doi.org/10.1158/1940-6207.CAPR-13-0181.
[10] D.M. Gilkes, G.L. Semenza, D. Wirtz, Hypoxia and the extracellular matrix: drivers of tumour metastasis, Nat. Rev. Canc. 14 (2014) 430–439, https://doi.org/10.1038/nrc3726.
[11] V. Tirino, V. Desiderio, F. Paino, A. De Rosa, F. Papaccio, M. La Noce, L. Laino, F. De Francesco, G. Papaccio, Cancer stem cells in solid tumors: an overview and new approaches for their isolation and characterization, Faseb. J. 27 (2013) 13–24, https://doi.org/10.1096/fj.12-218222.
[12] A. Pietras, A.M. Katz, E.J. Ekström, B. Wee, J.J. Halliday, K.L. Pitter, J.L. Werbeck, N.M. Amankulor, J.T. Huse, E.C. Holland, Osteopontin-CD44 signaling in the glioma perivascular niche enhances cancer stem cell phenotypes and promotes aggressive tumor growth, Cell Stem Cell. 14 (2014) 357–369, https://doi.org/10.1016/j.stem.2014.01.005.
[13] L. a. Shevde, R.S. Samant, Role of osteopontin in the pathophysiology of cancer, Matrix Biol. 37 (2014) 131–141, https://doi.org/10.1016/j.matbio.2014.03.001.
[14] H.C. Kwaan, A.P. Mazar, B.J. Mcmahon, The apparent uPA/PAI-1 paradox in Cancer : more than meets the eye, Semin. Thromb. Hemost. 39 (2013) 382–391.
[15] B.W. Robertson, L. Bonsal, M. a Chellaiah, Regulation of Erk1/2 activation by osteopontin in PC3 human prostate cancer cells, Mol. Canc. 9 (2010) 260, https://doi.org/10.1186/1476-4598-9-260.
[16] B. Zhang, C. Yin, H. Li, L. Shi, N. Liu, Y. Sun, S. Lu, Y. Liu, L. Sun, X. Li, W. Chen, Y. Qi, Nir1 promotes invasion of breast cancer cells by binding to chemokine (C-C motif) ligand 18 through the PI3K/Akt/GSK3β/Snail signalling pathway, Eur. J. Canc. 49 (2013) 3900–3913, https://doi.org/10.1016/j.ejca.2013.07.146.
[17] M.U. Romer, L. Larsen, H. Offenberg, N. Brunner, U.A. Lademann, Plasminogen activator inhibitor 1 protects fibrosarcoma cells from etoposide-induced apoptosis through activation of the PI3K/Akt cell survival pathway, Neoplasia 10 (2008) 1083–1091, https://doi.org/10.1593/neo.08486.
[18] J. Kang, W. Kim, T. Kwon, H. Youn, J.S. Kim, B. Youn, Plasminogen activator inhibitor-1 enhances radioresistance and aggressiveness of non-small cell lung cancer cells, Oncotarget 7 (2016), https://doi.org/10.18632/oncotarget.8208.
[19] L.M. Sholl, J.A. Barletta, B.Y. Yeap, L.R. Chirieac, J.L. Hornick, Sox2 protein expression is an independent poor prognostic indicator in stage I lung adenocarcinoma, Am. J. Surg. Pathol. 34 (2010) 1193–1198, https://doi.org/10.1097/PAS.0b013e3181e5e024.
[20] E. Park, S.Y. Park, P.-L. Sun, Y. Jin, J.E. Kim, S. Jheon, K. Kim, C.T. Lee, H. Kim, J.-H. Chung, E. Park, S.Y. Park, P.-L. Sun, Y. Jin, J.E. Kim, S. Jheon, K. Kim, C.T. Lee, H. Kim, J.-H. Chung, Prognostic significance of stem cell-related marker expression and its correlation with histologic subtypes in lung adenocarcinoma, Oncotarget 7 (2016) 42502–42512, https://doi.org/10.18632/oncotarget.9894.
[21] H. Peng, E.L. Herzog, Fibrocytes: emerging effector cells in chronic inflammation, Curr. Opin. Pharmacol. 12 (2012) 491–496, https://doi.org/10.1016/j.coph.2012.03.002.
[22] A. Andersson-Sjöland, C.G. de Alba, K. Nihlberg, C. Becerril, R. Ramírez, A. Pardo, G. Westergren-Thorsson, M. Selman, Fibrocytes are a potential source of lung fibroblasts in idiopathic pulmonary fibrosis, Int. J. Biochem. Cell Biol. 40 (2008) 2129–2140, https://doi.org/10.1016/j.biocel.2008.02.012.
[23] M. Kraman, P.J. Bambrough, J.N. Arnold, E.W. Roberts, L. Magiera, J.O. Jones, A. Gopinathan, D. a Tuveson, D.T. Fearon, Suppression of antitumor immunity by stromal cells expressing fibroblast activation protein-alpha, Science 330 (2010) 827–830, https://doi.org/10.1126/science.1195300.
[24] H. Zhang, I. Maric, M.J. DiPrima, J. Khan, R.J. Orentas, R.N. Kaplan, C.L. Mackall, Fibrocytes represent a novel MDSC subset circulating in patients with metastatic cancer, Blood 122 (2013) 1105–1113, https://doi.org/10.1182/blood-2012-08-449413.
[25] H.W. van Deventer, D.A. Palmieri, Q.P. Wu, E.C. McCook, J.S. Serody,

Circulating fibrocytes prepare the lung for cancer metastasis by recruiting Ly-6C+ monocytes via CCL2, J. Immunol. 190 (2013) 4861–4867, https://doi.org/10.4049/jimmunol.1202857.
[26] T. Oskarsson, E. Batlle, J. Massagué, Metastatic stem cells: sources, niches, and vital pathways, Cell Stem Cell. 14 (2014) 306–321, https://doi.org/10.1016/j.stem.2014.02.002.
[27] J. Paulsson, P. Micke, Prognostic relevance of cancer-associated fibroblasts in human cancer, Semin. Canc. Biol. 25 (2014) 61–68, https://doi.org/10.1016/j.semcancer.2014.02.006.
[28] Y. Aono, M. Kishi, Y. Yokota, M. Azuma, K. Kinoshita, A. Takezaki, S. Sato, H. Kawano, J. Kishi, H. Goto, H. Uehara, K. Izumi, Y. Nishioka, Role of platelet-derived growth factor/platelet-derived growth factor receptor axis in the trafficking of circulating fibrocytes in pulmonary fibrosis, Am. J. Respir. Cell Mol. Biol. 51 (2014) 793–801, https://doi.org/10.1165/rcmb.2013-0455OC.
[29] G. Ishii, T. Sangai, T. Oda, Y. Aoyagi, T. Hasebe, N. Kanomata, Y. Endoh, C. Okumura, Y. Okuhara, J. Magae, M. Emura, T. Ochiya, A. Ochiai, Bone-marrow-derived myofibroblasts contribute to the cancer-induced stromal reaction, Biochem. Biophys. Res. Commun. 309 (2003) 232–240, https://doi.org/10.1016/S0006-291X(03)01544-4.
[30] C. Raggi, H.S. Mousa, M. Correnti, A. Sica, P. Invernizzi, Cancer stem cells and tumor-associated macrophages: a roadmap for multitargeting strategies, Oncogene 35 (2016) 671–682, https://doi.org/10.1038/onc.2015.132.
[31] J.G. Quatromoni, E. Eruslanov, Tumor-associated macrophages: function, phenotype, and link to prognosis in human lung cancer, Am. J. Transl. Res. 4 (2012) 376–389 doi:2012;4(4):376–389.
[32] T. Kisseleva, M. Von Köckritz-Blickwede, D. Reichart, S.M. McGillvray, G. Wingender, M. Kronenberg, C.K. Glass, V. Nizet, D.A. Brenner, Fibrocyte-like cells recruited to the spleen support innate and adaptive immune responses to acute injury or infection, J. Mol. Med. 89 (2011) 997–1013, https://doi.org/10.1007/s00109-011-0756-0.
[33] D. Peng, T. Tanikawa, W. Li, L. Zhao, L. Vatan, W. Szeliga, S. Wan, S. Wei, Y. Wang, Y. Liu, E. Staroslawska, F. Szubstarski, J. Rolinski, E. Grywalska, A. Stanis??awek, W. Polkowski, A. Kurylcio, C. Kleer, A.E. Chang, M. Wicha, M. Sabel, W. Zou, I. Kryczek, Myeloid-derived suppressor cells endow stem-like qualities to breast cancer cells through IL6/STAT3 and NO/NOTCH cross-talk signaling, Canc. Res. 76 (2016) 3156–3165, https://doi.org/10.1158/0008-5472.CAN-15-2528.
[34] C.M. Diaz-Montero, J. Finke, A.J. Montero, Myeloid-derived suppressor cells in cancer: therapeutic, predictive, and prognostic implications, Semin. Oncol. 41 (2014) 174–184, https://doi.org/10.1053/j.seminoncol.2014.02.003.
[35] Y. Shi, L. Ou, S. Han, M. Li, M.M.O. Pena, E. a Pena, C. Liu, M. Nagarkatti, D. Fan, W. Ai, Deficiency of Kruppel-like factor KLF4 in myeloid-derived suppressor cells inhibits tumor pulmonary metastasis in mice accompanied by decreased fibrocytes, Oncogenesis 3 (2014) e129, https://doi.org/10.1038/oncsis.2014.44.
[36] K. Xu, X. Tian, S.Y. Oh, M. Movassaghi, S.P. Naber, C. Kuperwasser, R.J. Buchsbaum, The fibroblast Tiam1-osteopontin pathway modulates breast cancer invasion and metastasis, Breast Cancer Res. 18 (2016) 14, https://doi.org/10.1186/s13058-016-0674-8.
[37] M. Todaro, M. Gaggianesi, V. Catalano, A. Benfante, F. Iovino, M. Biffoni, T. Apuzzo, I. Sperduti, S. Volpe, G. Cocorullo, G. Gulotta, F. Dieli, R. De Maria, G. Stassi, CD44v6 is a marker of constitutive and reprogrammed cancer stem cells driving colon cancer metastasis, Cell Stem Cell. 14 (2014) 342–356, https://doi.org/10.1016/j.stem.2014.01.009.
[38] G. Rao, H. Wang, B. Li, L. Huang, D. Xue, X. Wang, H. Jin, J. Wang, Y. Zhu, Y. Lu, L. Du, Q. Chen, Reciprocal interactions between tumor-associated macrophages and CD44-positive cancer cells via osteopontin/CD44 promote tumorigenicity in colorectal cancer, Clin. Canc. Res. 19 (2013) 785–797, https://doi.org/10.1158/1078-0432.CCR-12-2788.
[39] T. Ploenes, B. Scholtes, A. Krohn, M. Burger, B. Passlick, J. Müller-Quernheim, G. Zissel, CC-Chemokine ligand 18 induces epithelial to mesenchymal transition in lung cancer A549 cells and elevates the invasive potential, PLoS One 8 (2013), https://doi.org/10.1371/journal.pone.0053068.
[40] S. Su, Q. Liu, J. Chen, J. Chen, F. Chen, C. He, D. Huang, W. Wu, L. Lin, W. Huang, J. Zhang, X. Cui, F. Zheng, H. Li, H. Yao, F. Su, E. Song, A Positive feedback loop between mesenchymal-like cancer cells and macrophages is essential to breast cancer metastasis, Canc. Cell 25 (2014) 605–620, https://doi.org/10.1016/j.ccr.2014.03.021.
[41] T. Plönes, A. Krohn, M. Burger, H. Veelken, B. Passlick, J. Müller-Quernheim, G. Zissel, Serum level of CC-chemokine ligand 18 is increased in patients with non-small-cell lung cancer and correlates with survival time in adenocarcinomas, PLoS One 7 (2012) 1–7, https://doi.org/10.1371/journal.pone.0041746.
[42] S. a. Mani, W. Guo, M.J. Liao, E.N. Eaton, A. Ayyanan, A.Y. Zhou, M. Brooks, F. Reinhard, C.C. Zhang, M. Shipitsin, L.L. Campbell, K. Polyak, C. Brisken, J. Yang, R. a. Weinberg, The epithelial-mesenchymal transition generates cells with properties of stem cells, Cell 133 (2008) 704–715, https://doi.org/10.1016/j.cell.2008.03.027.
[43] P.J. Declerck, A. Gils, Three decades of research on plasminogen activator inhibitor-1: a multifaceted serpin, Semin. Thromb. Hemost. 39 (2013) 356–364, https://doi.org/10.1055/s-0033-1334487.
[44] R.D. Balsara, V.A. Ploplis, Plasminogen activator inhibitor-1: the double-edged sword in apoptosis, Thromb. Haemostasis 100 (2008) 1029–1036, https://doi.org/10.1160/TH08-07-0427.